COO-1549-10

Technical Progress Report

NUCLEAR PHYSICS STUDIES USING NUCLEAR EMULSIONS

Contract Number AT (11-1)-1549

November 1, 1968 through October 31, 1969

between

The United States Atomic Energy Commission

and the

University of Wyoming, Laramie, Wyoming

DISCLAIMER

I. Introduction

This report summarizes the work carried out during the past year under the Contract AT (11-1)-1549 between the University of Wyoming and the U. S. Atomic Energy Commission. Work in the development of instrumentation at the University of Wyoming for use in experiments to be done at the University of Colorado Cyclotron is included. Work completed on the analysis of experiments done at the Berkeley heavy ion accelerator is discussed.

II. Beam Transport System

W. G. Simon, H. B. Eldridge, R. J. Jiacoletti, S. T. Ahrens

A schematic of the present beam transport system is shown in Figure II-1. The rigidity and line-up technique have both been improved and the background sources have been effectively reduced.

The rigidity was improved by taking the scattering chamber off a tripod support subject to floor vibrations and suspending it from the overhead I-beam to which the rest of the transport system is attached. Horizontal torsional movement was eliminated through the use of steel cables.

The line-up technique has also been improved, and our basic line-up procedure consists of two steps. First, we make an optical line-up using a pentaprism which is viewed with a transit. Light sources are then viewed up-beam close to the cyclotron and down-beam in the scattering chamber. Since this procedure does not eliminate the possibility of a slight bend in the beam at the pentaprism, the pentaprism was placed close to the 1^{0} bending magnet. The second step in the line-up procedure is made with an actual beam. A carbon target coated with a phosphor is placed in the beam line at a dip of 45^{0}. This target is then viewed through the plexiglas window on the top of the chamber by means of a TV camera. When line-up is achieved, the beam is not disturbed other than stopping it with a flag. The carbon target is then replaced by the desired target, the emulsions are placed around the scattering chamber as shown in Figure II-2, and the exposure made. To aid in the line-up, several collimators have been used as designated in Figure II-1.

Figure II-1

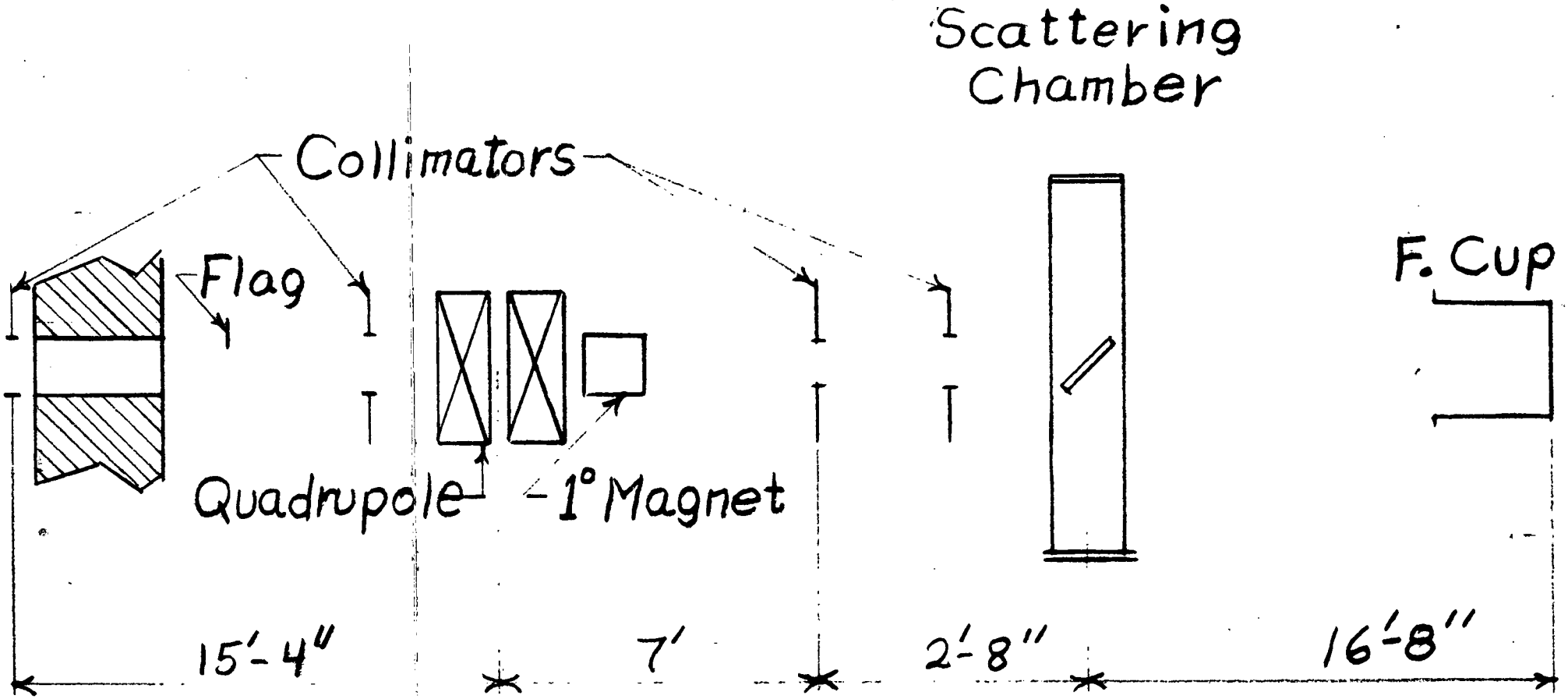
Scattering
Chamber
Collimators
Flag
F. Cup
Quadrupole
1° Magnet
15'-4"
7'
2'-8"
16'-8"

Figure II-2

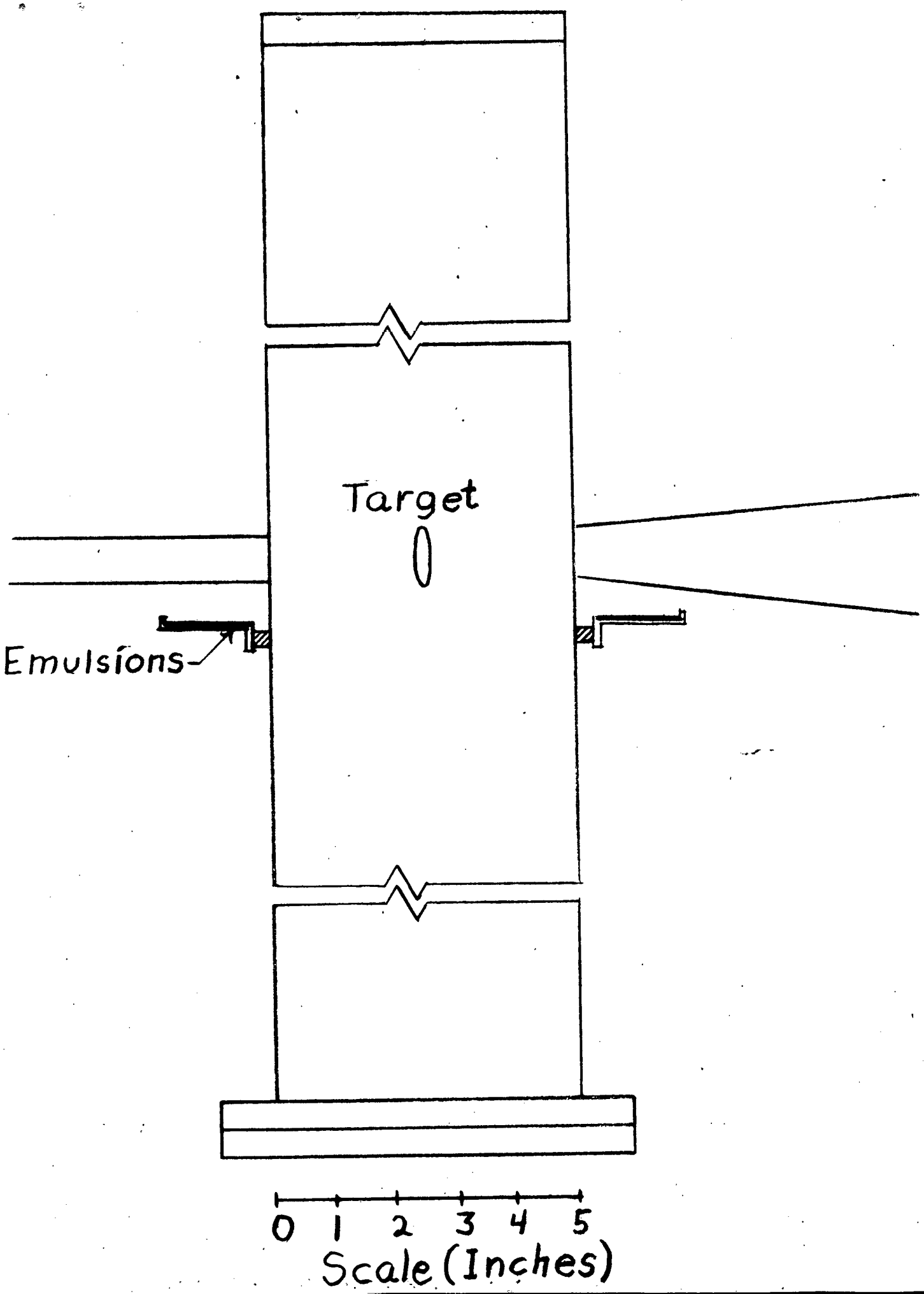

III. Neutron Spectra from Charged Particle Reactions

W. G. Simon, S. T. Ahrens, H. B. Eldridge

Our present goal has been to obtain neutron spectra from the following four reactions: (1) 26.0 MeV Protons on Cu^{63}, (2) 26.0 MeV Protons on Ni^{60}, (3) 31.3 MeV α's on Cu^{63} and (4) 31.3 MeV α's on Ni^{60}. While these four reactions have at least one parameter in common with one another, reactions (1) and (4) both yield the same compound nucleus and excitation energy. Thus any angular difference in the neutron spectra from these two reactions can be related to the different angular momenta of these two systems.

Thus far reactions (1) and (2) have been run and the nuclear emulsions scanned. Figure III-1 shows a Le Couteur plot for the neutron spectra from reaction (1). Figure III-2 shows the CM energy-angular distribution for the same reaction. In this we compare the measured spectra with statistical model calculating. These calculations include the effects of multiple particle emission and of angular momentum. Above 6 MeV neutron energy there is a pronounced forward peaking in the angular distributions, with a forward to backward ratio of about four at 10 MeV. Below 6 MeV the spectra are nearly symmetric about 90^{o} and in good agreement with the calculations except for an absolute normalization discrepancy: The experimental values are 15% below the calculated ones. A preliminary run has been made for reaction (3). The beam energy as determined by scattering at 90^{o} from gold was several MeV low and will have to be adjusted before a final run can be made for this reaction.

The use of a fairly thick target gives rise to significant multiple scattering. This scattered beam would give rise to background when it hit the exit tube. To eliminate this, the cylindrical shaped exit tube was replaced by a cone shaped design as seen in Figure II-2. Multiple scattering also necessitates a correction in the charge collected in the Faraday cup. Some particles are scattered outside the cup entrance. Measurements of the beam profile at the Faraday cup were made by activating a copper foil, cutting it into small pieces and measuring the activity on each piece. The results were in excellent agreement with calculations according to Moliere's theory, and we feel confident that corrections for multiple scattering can be calculated reliably.

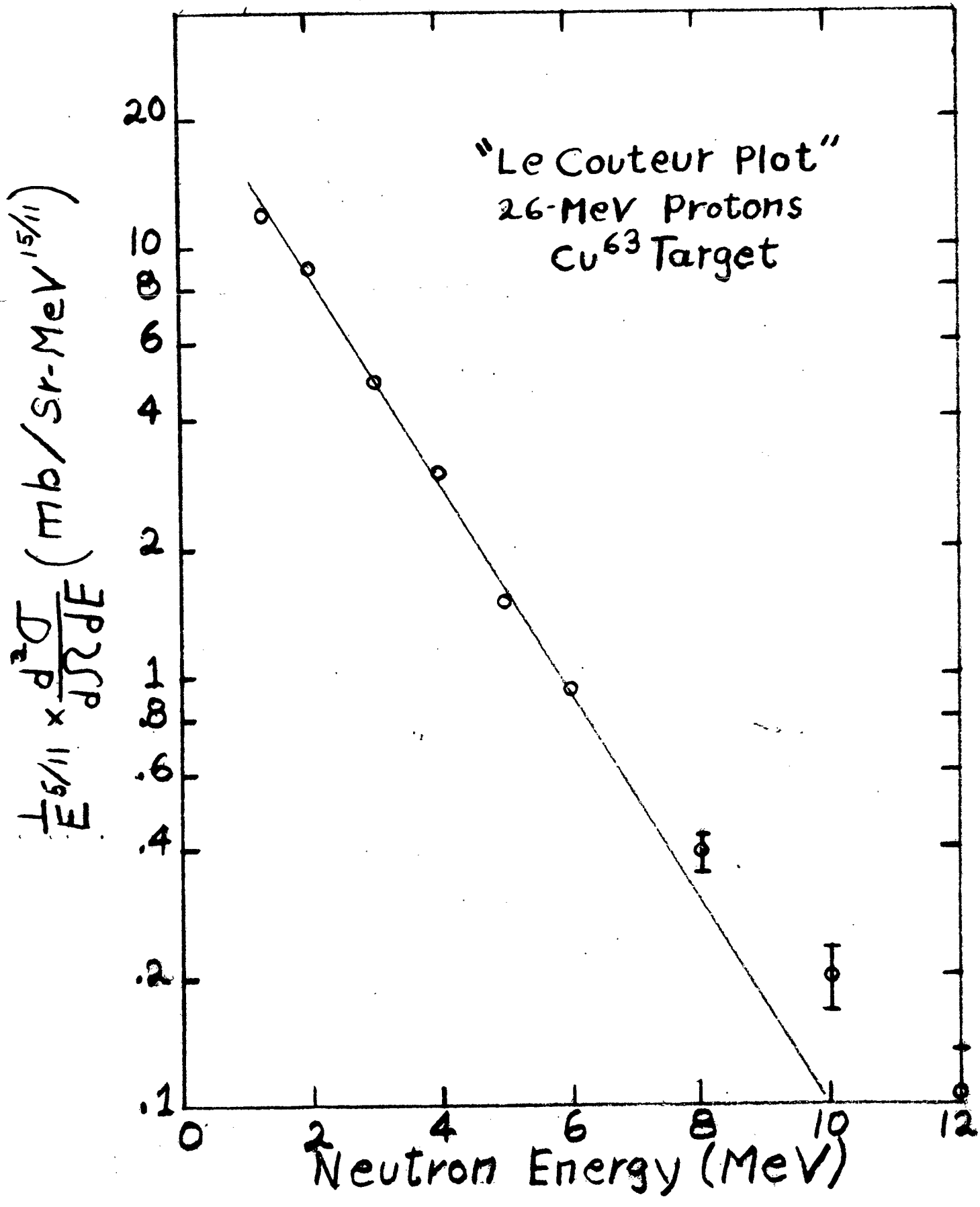
"Le Couteur Plot"
26-MeV Protons
Cu63 Target
$\frac{1}{E^{5/11}} \times \frac{d^2\sigma}{d\Omega dE}$ (mb/Sr-MeV$^{15/11}$)
20
10
8
6
4
2
1
.8
.6
.4
.2
.1
0
2
4
6
8
10
12
Neutron Energy (MeV)

Figure III-1

Figure III-2

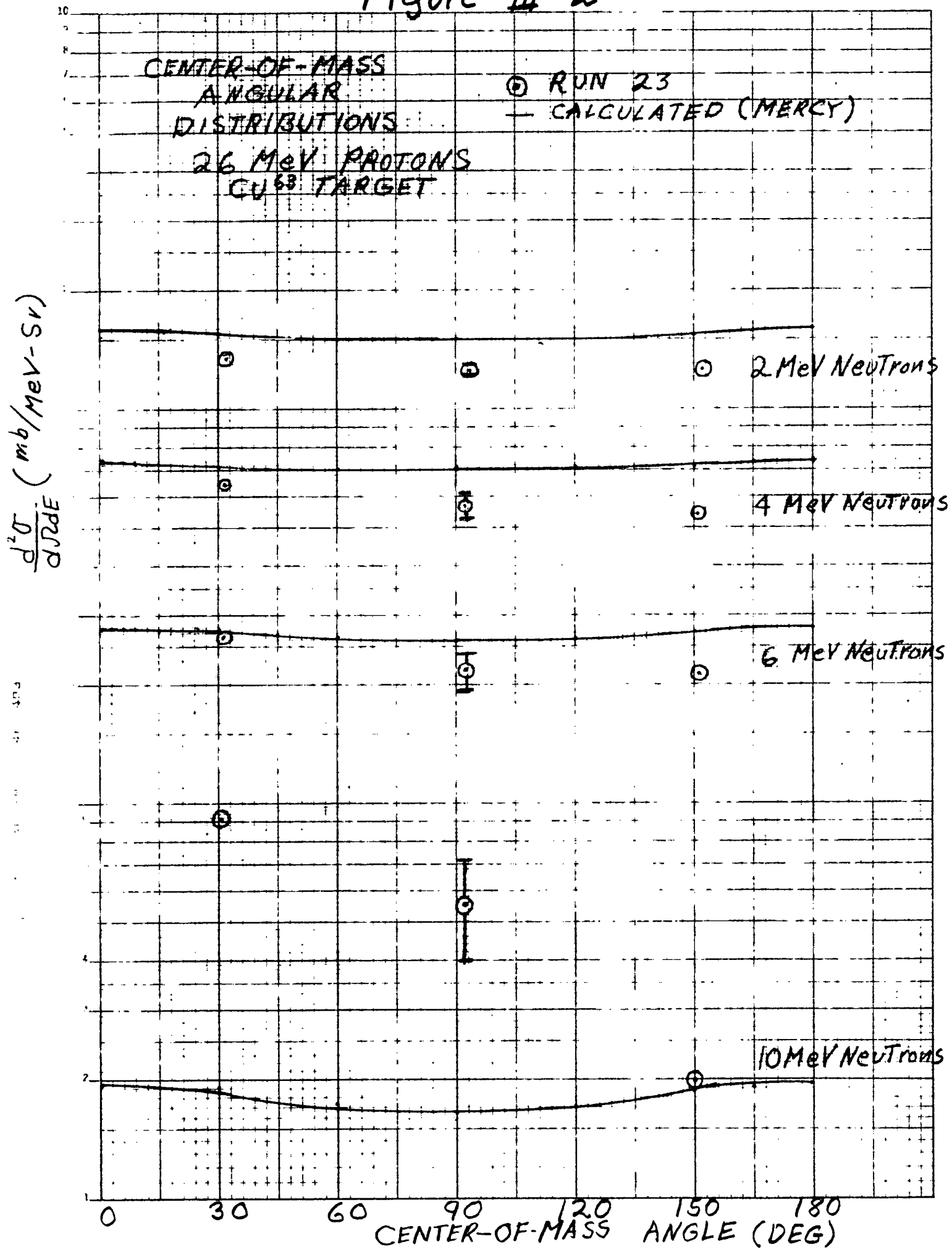
CENTER-OF-MASS
ANGULAR
DISTRIBUTIONS
26 MeV PROTONS
Cu⁶³ TARGET
RUN 23
CALCULATED (MERCY)
2 MeV NeuTrons
4 MeV NeuTrons
6 MeV NeuTrons
10 MeV NeuTrons
d²σ/dΩdE (mb/MeV-Sr)
0
30
60
90
120
150
180
CENTER-OF-MASS ANGLE (DEG)

IV. Neutron Spectrometer Construction

H. B. Eldridge — University of Wyoming
C. S. Zaidins — University of Colorado

A. Efficiency Studies

In the interest of improving the efficiency of the double scintillator neutron time-of-flight spectrometer described in the 1967 progress report, a study had been made of the time structure of the beam from the University of Colorado cyclotron. It is well known that the beam from a cyclotron is composed of pulses of particles whose width is determined by the phase acceptance and whose repetition rate is determined by the frequency of the Dee voltage. This study was initiated to test the feasibility of a suggestion by Professor D. A. Lind at the University of Colorado that one could utilize this microstructure of the beam by picking off a timing pulse from the Radio Frequency (RF) voltage on the Dees of the cyclotron that would have a constant time relationship to the cyclotron beam pulses. Professor Lind also felt that the time width of the beam pulses was sufficiently small that neglible error would be introduced due to the resulting uncertainty in what part of the beam pulse the interacting proton was located.

Consequently an experiment was designed which would measure the time width of the cyclotron beam bursts plus the jitter associated with the method of pick-off so as to compare with the time dispersion introduced by the neutron detector. It is to be realized that if the suggestion was practical that the first scintillator of the present spectrometer could be eliminated hence increasing the efficiency by the macroscopic (n,p) cross-section for the first scintillator. The detector (which will take the place of the second scintillator in the first design) was a 2" diameter by 2" high fast plastic scintillator coupled to a 56 AVP phototube with a commercially available tubebase, preamplifier, and fast discriminator (ORTEC 268). Two such assemblies

were available and they will be referred to as detector 1 and detector 2. Pulses from fast discriminator in the tube bases served as start pulses for the time-to-amplitude converter (TAC) while a start pulse was derived from the cyclotron radio frequency voltage which drove the Dee structure.

The method consisted of measuring the width of the peak in the TAC spectrum for three experimental configurations.

1) The two detectors were placed facing each other with a Co^{60} source in between. Since Co^{60} furnishes a two member γ-cascade, a pulse of one member of the cascade in a detector served as a start pulse to the TAC while the other member of the cascade, detected by the other detector, served, after a suitable delay, as a stop pulse for the TAC. The width of the peak in the TAC spectrum was then due to the time jitter in both detectors plus the TAC and will be called W_{12}.

2) Detector 1 was placed 1 meter from a thick magnesium target which was bombarded with 26 MeV protons from the cyclotron. For this measurement, the stop pulse was derived from the RF voltage while the start pulse was furnished by the prompt γ-rays coming from the target at 90^{o} onto detector 1. The width of the peak in the TAC spectrum will be called W_{b1}.

3) The experiment is the same except detector 2 replaces detector 1, and the width of the peak is W_{b2}.

If the assumption is made that the contribution to the total width of each element adds as the square root of the sum of the squares, the time jitter introduced by detector 1, detector 2 and the beam may be determined. The three experimental numbers W_{12}, W_{b1} and W_{b2} are related to W_b, W_1, and W_2 (the time dispersion introduced by the finite width of the beam burst and the method of pick-off, detector 1, and detector 2 respectively) as follows:

$$W_{12} = W_{.}^{2} + W_2^2 \text{ , } W_{b1} = W_b^2 + W_1^2 \text{ , } W_{b2} = W_b^2 + W_2^2$$

Our preliminary results on the microstructure of the cyclotron beam for 26 MeV protons are as shown in Table IV-1.

Table IV-1

Beam Burst Width

University of Colorado Cyclotron, 26 MeV Protons

W_{12}	1.13 nsec	W_b	0.62 nsec
W_{b1}	1.16 nsec	W_1	0.92 nsec
W_{b2}	0.94 nsec	W_2	0.76 nsec

During these preliminary runs, the above measured widths did not seem to be very sensitive to tuning of the RF oscillator.

The use of the above method to measure the energy of neutrons emitted from the target suffers from a lack of dynamic range. The beam bursts were separated by ~ 50 nsec; hence, the flight times measurable for the neutrons must be less than 50 nsec. To alleviate this problem, a program is in progress by staff members at the cyclotron to vary the rate at which the beam bursts strike the target. It is also planned to extend the above measurements to beams of different particles as well as different operating conditions of the cyclotron to determine if the microstructure of the beam remains well enough defined in time to be useful for time-of-flight work.

B. γ - Background Reduction

Our preliminary measurements of neutron time-of-flight spectra at the University of Colorado Cyclotron indicated a need for some sort of γ background suppression. Conventional pulse shape discrimination was chosen as the most practical solution and the initial experiments indicated that a medium energy resolution recoil spectrometer was possible if use was made of pulse height as well as pulse shape information in the scintillator. Also during

the design stages of the individual neutron detector a conventional PuBe neutron source[1] was utilized to such an extent that, in the interest of compliance with the maximum permissible exposure regulations, it was felt that the dose rate from the source should be determined. However, to obtain an estimate of the biological dose due to neutrons, one must first determine the energy spectrum of the neutrons since the factor which converts neutron flux density to dose depends upon the neutron energy.

There are numerous measurements of the energy spectrum of neutrons from PuBe sources available in the literature and at least the more recent ones appear to show consistency.[2,3,4,5,6] Also, some recent calculations using the known cross sections for the $^{9}Be(\alpha,n)^{12}C$ reactions have been quite successful in explaining the major features of the spectrum.[5,6,7] In most of the calculations, however, the effects of the ^{241}Pu contamination, ^{239}Pu fission and various neutron interactions with Beryllium have been neglected. It has been mentioned that the ^{241} contamination could cause a 11.1 MeV neutron group whose intensity would increase by about 1% per year of source life. The relative importance of the secondary neutron reactions in the source may be expressed as the percentage of neutrons affected. Such considerations[6] have led to the following estimates: ^{9}Be elastic scattering, 30%; (n,2n) reactions, 6%; (n, fission) reactions, 3%. Past measurements of the flux density from PuBe sources have found in addition a large spatial anistropy with respect to the cylindrical axis of the source.[5,8]

The above mentioned effects which tend to modify the neutron energy spectrum would depend upon the size, method of construction, and age of the neutron source, thereby indicating that considerable variation in the neutron energy spectrum could be found for different sources and for a given source at different times. In view of this possible variation, it was decided to measure the fast neutron spectrum from the PuBe source used in the neutron time-of-flight experiments, in a similar geometrical arrangement, so as to arrive at an

estimate of the fast neutron dose one could expect working on that experiment.

The neutron spectrometer was of the proton recoil type in which an organic liquid scintillator[9] viewed by a photomultiplier tube[10] served as both radiator and detector of the recoiling protons. The rather intense γ-ray background was suppressed by conventional zero cross pulse shape discrimination. This suppression of γ-ray response is accomplished by taking advantage of the difference in the ratio of slow decay component to total amount of light emitted by the liquid scintillator for recoil electrons and recoil protons.[11] The recoil protons have a larger amount of slow component for a given total amount of light output; hence, if the current pulse from a photomultiplier tube viewing the scintillator is integrated with a suitable time constant, the resultant pulse will have a slower rise time for recoiling proton pulses than for recoiling electron pulses. By differentiating this pulse twice, a bipolar shaped pulse is obtained where the time interval from leading edge to zero cross point will be longer for recoil proton pulses than for recoil electron pulses. This time difference ($\sim$ 25 nsec) is easily resolved by most modern time-to-amplitude converters where the start output is derived from somewhere on the leading edge of the pulse.

The spectrometer components are shown schematically in Figure IV-1 where the current pulse from dynode 11 of the 14 stage tube is integrated by a charge sensitive preamplifier and then shaped by a double delay line clipping in the following linear amplifier. The bipolar output from the linear amplifier is split so that one branch leads to the pulse height analyzer through a suitable delay to satisfy the time relationship between linear and gate pulse required by the analyzer. The other branch of the dynode 11 signal is presented to a timing single channel analyzer which serves as both an integral discriminator and a generator of fast timing pulse at the zero cross point of the bipolar pulse. This timing pulse serves as a stop pulse to the time-to-amplitude converter. The start pulse for the time-to-amplitude converter is derived from dynode 14

through a standard inductive time pick-off, fast amplifier, tunnel diode discriminator and delay so as to place the time spectrum of zero crossings about mid-scale for 125 nsec full scale conversion. A typical time spectrum of zero crossings is shown in Figure IV-2, where the discriminators are set at 800 KeV electron energy which corresponds to about 2.6 MeV proton energy. The output from a single channel analyzer, whose window is set on one of the peaks in the time-to-amplitude converter spectrum, then allows one to store either recoil pulses due to γ-rays or due to neutrons by gating the pulse height analyzer, which is storing the recoil spectrum from the linear amplifier. Other methods of pulse shape discrimination[12] allow one to discriminate between much lower energy neutrons and γ-rays, but all the components of the above mentioned system are standard modules which are normally available in a nuclear physics laboratory. A liquid scintillator was chosen over stilbene since a much larger volume can be obtained, thereby increasing the efficiency.

The output from the spectrometer is one of three spectra: a spectrum of times to cross zero from the time-to-amplitude converter, a recoil electron spectrum from Compton scattered γ-rays, or a recoil proton spectrum due to n,p scattering of the incident neutrons. All three spectra are used in the determination of an arbitrary neutron energy spectrum. The incident neutron energy spectrum may be obtained from the recoil proton energy spectrum by the following expression:[13]

$$N_0(E) = - \frac{dN_p(E)}{dE} \frac{E}{n\sigma(E)}$$

where

$N_0(E)$ = the desired neutron energy spectrum

$N_p(E)$ = the recoil proton energy spectrum

E = the energy

$\sigma(E)$ = n,p elastic cross section

n = Hydrogen atom density per cm^2

The above experssion assumes the n,p cross section isotropic in the center of mass and neglects multiple scattering, finite radiator size, and neutron

interactions in the scintillator other than n,p elastic scattering.

The energy response of the liquid scintillator used in this experiment had been determined for both electrons and protons.[14] Using the data from Reference 14, the following expression was determined for energy calibration of the pulse height analyzer:

For $E_p < 8$ MeV,

$$E_p = \frac{-0.215 + (0.0462 + 0.112 \frac{dE}{dC} C (C-C_0))^{\frac{1}{2}}}{0.056} \quad (2)$$

For $E_p \leq 8$ MeV

$$E_p = \frac{1.28 + \frac{dE}{dC} C (C-C_0)}{0.60} \quad (3)$$

Here,

E_p = the proton energy

E_C = the electron energy

$\frac{dE}{dC} C$, C_0 = the slope, intercept of the calibration of pulse height analyzer using the Compton edges of known energy of γ-rays

C = the channel number on the pulse height analyzer

With the neutron source in its paraffin shield, two suitable gamma rays were obtained for the energy calibration of the pulse height analyzer: the 2.225 MeV gamma ray from neutron capture in the paraffin and the 4.43 MeV gamma ray from the isomeric transition of the first excited state to the ground state of the ^{12}C in the source formed from the reaction $^{9}Be(^{4}He,n)^{12}C$. The Compton edges of the two calibration gamma rays are shown in Figure IV-3 where, since the organic scintillator used in this experiment is composed of low atomic number material, the photopeaks are absent.

Typical neutron energy spectra from this PuBe source obtained by applying equation (1) to recoil proton spectra using the Philco 2000 computer system at the University of Wyoming are shown in Figure IV-4. The errors in the measurements due to counting statistics are smaller than the size of the points. The shielded curve refers to the PuBe source being inside a 7 inch thick paraffin shield, see Figure IV-5, while the unshielded curve refers to

the source outside the shield. Referring again to Figure IV-5, position 1 indicates that the detector was located 40 cm. from the source in the plan of symmetry perpendicular to the cylindrical axis of the source. One can see from Figure IV-4 the effect of the paraffin shield which is the normal place the source is kept when not in use. Figure IV-6 shows the spectra obtained with the source outside the shield but with the detector at two different locations. Position 2 indicates that the detector was located 40 cm. from the source along the axis of cylindrical symmetry, as can be seen from Figure IV-5. The asymmytric spatial distribution of the flux density which was mentioned earlier is evident, and it appears that the asymmetry is greater for the lower energy neutrons, which is expected. For the source inside the paraffin shield this spatial asymmetry of the flux density was not observed.

Integration of the neutron energy distributions, such as Figures IV-5 and IV-6, over energy so as to obtain the total neutron flux density at 40 cm. from the source leads to the following results: in shield position 1, 36.1 ± .5; in shield position 2, 35.6 ± .5; out of shield position 1, 58.4 ± .5; out of shield position 2, 49.1 ± .5 neutrons/cm^2 sec. From these flux density measurements, a total yield of the source above 2.6 MeV is about 1 X 10^6 neutrons/sec., which compares favorably with other measurements on similar sources.

Using the table of flux density required to give the maximum permissible exposure of 100 mrem per 40 hour week as a function of neutron energy,[15] one can compute the dose rate and hence the time required for a worker to receive the maximum permissible exposure level from this PuBe source due to neutrons whose energy is greater than 2.6 MeV. The dose rate from the source, under the varying conditions of the experiment which are discussed above, was as follows: in shield position 1 or 2, 4.86; unshielded position 1, 8.07; unshielded position 2, 6.80 mrem/hr. For the permissible working time computation the fraction of maximum permissible exposure was determined for each energy interval of the measured neutron energy spectra, such as Figures IV-4 and IV-6, and the

fractions were then summed over the energy range. The total fraction of maximum permissible exposure was then used to obtain the time required for a worker to receive the maximum permissible exposure each 40 hour week as follows: in shield position 1 or 2, 20.6 hours; unshielded position 1, 12.4 hours; unshielded position 2, 14.7 hours. Based on the above the investigators conclude that considerable variation in neutron flux density can occur for different PuBe sources and the practice of calibrating neutron survey meters using such sources should be exercised with caution.

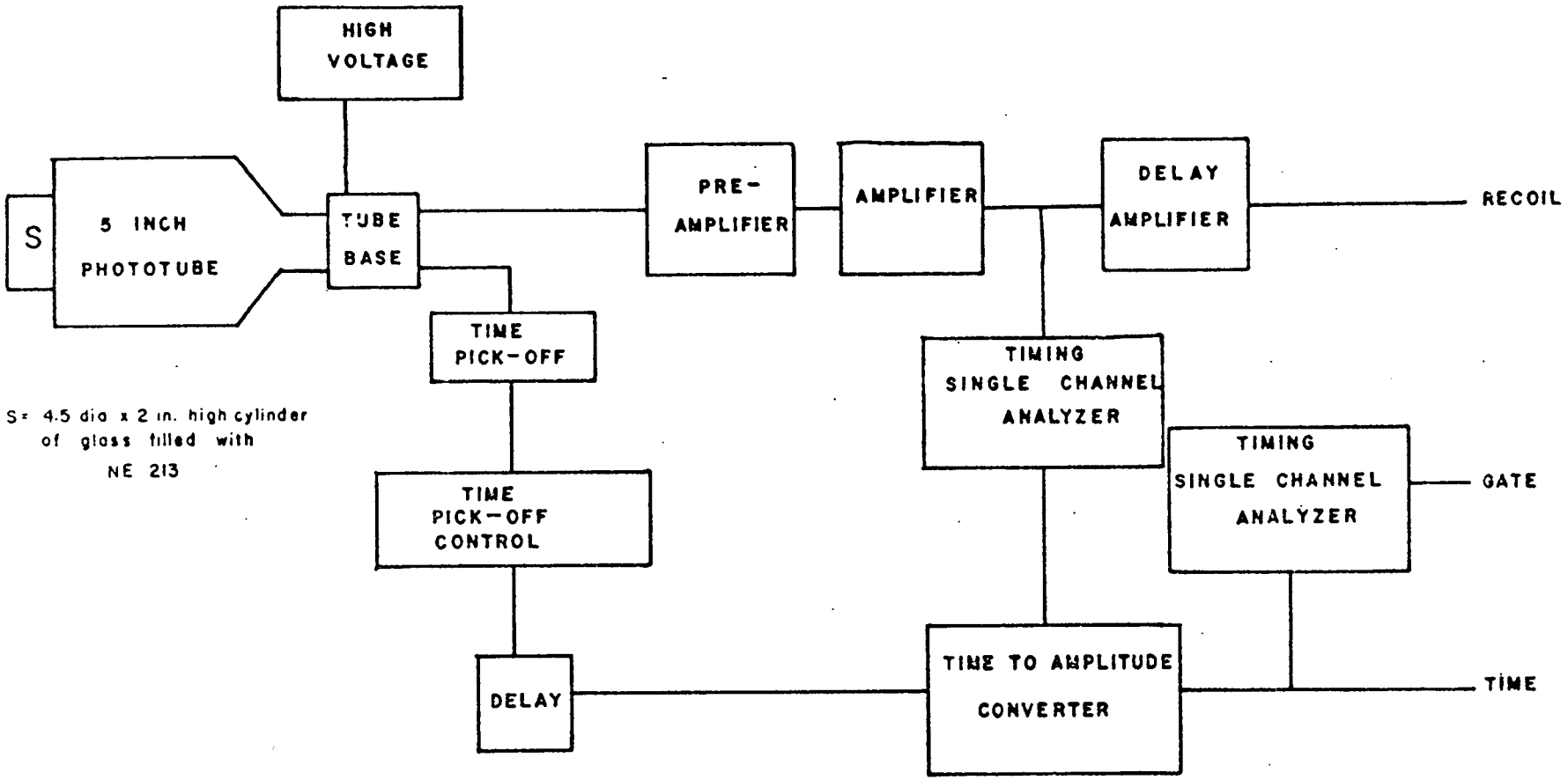

RECOIL NEUTRON SPECTROMETER

FIGURE IV-1

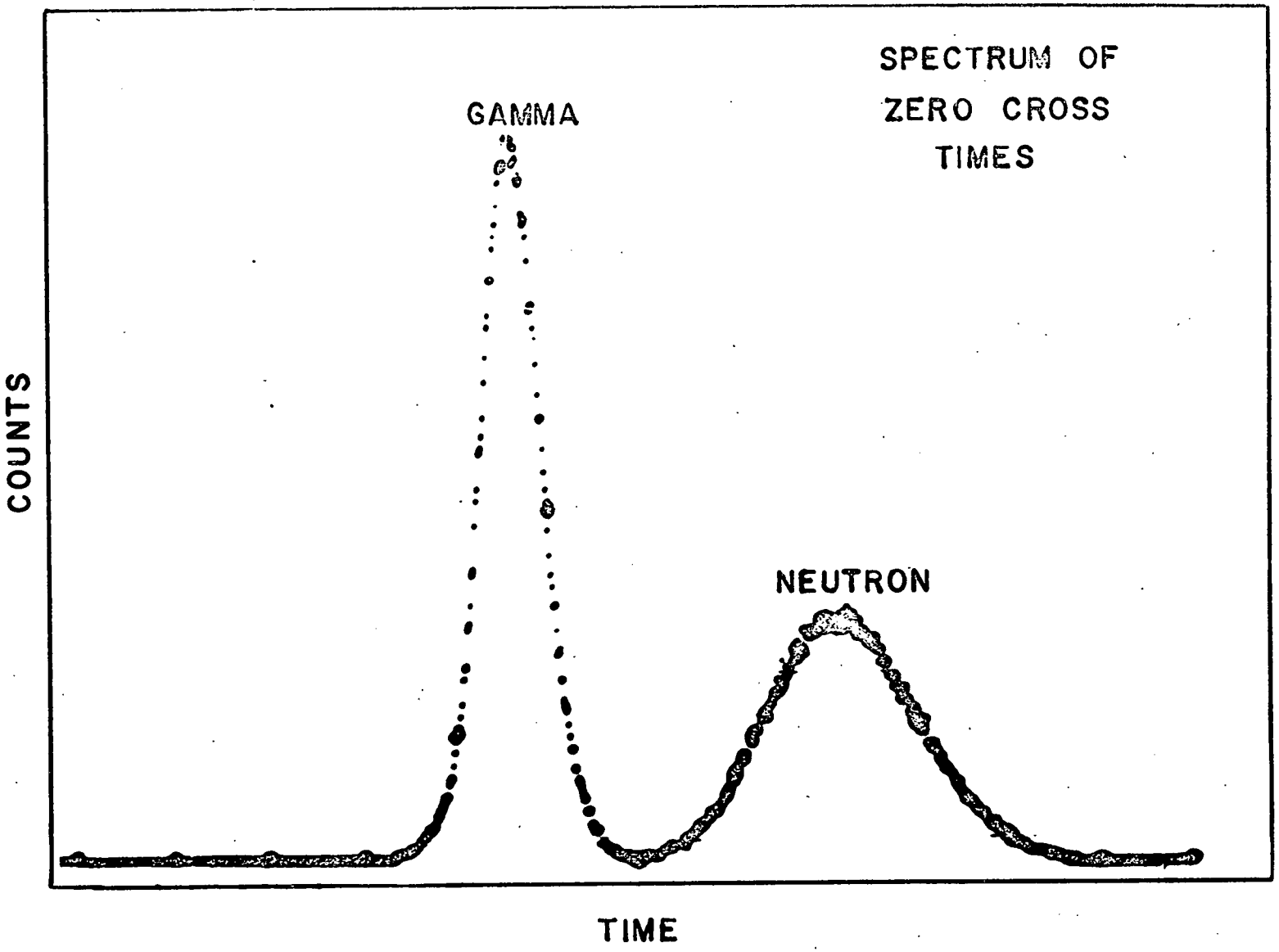

FIGURE IV-2

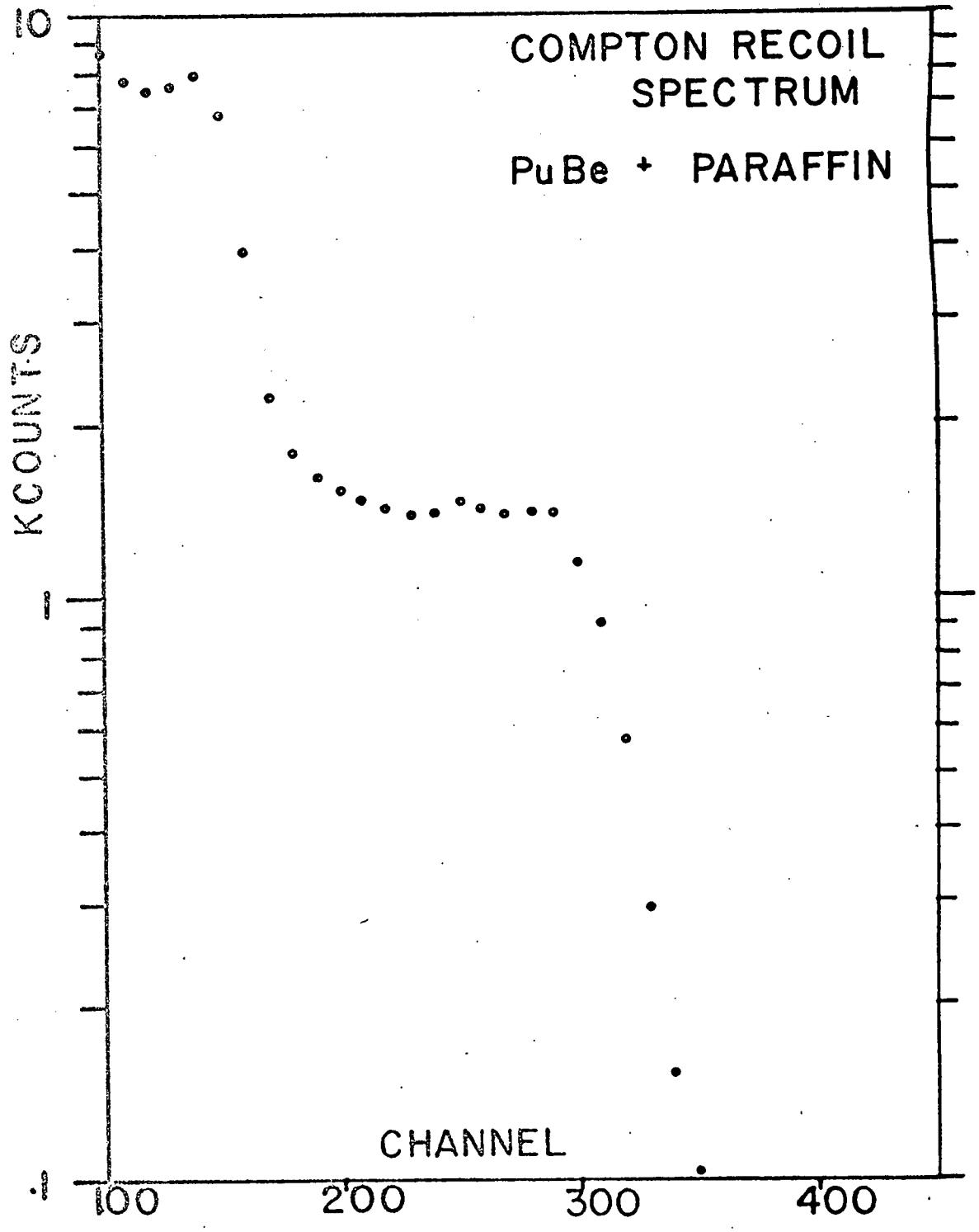
COMPTON RECOIL
SPECTRUM
PuBe + PARAFFIN
KCOUNTS
CHANNEL
100
200
300
400

figure iv-3

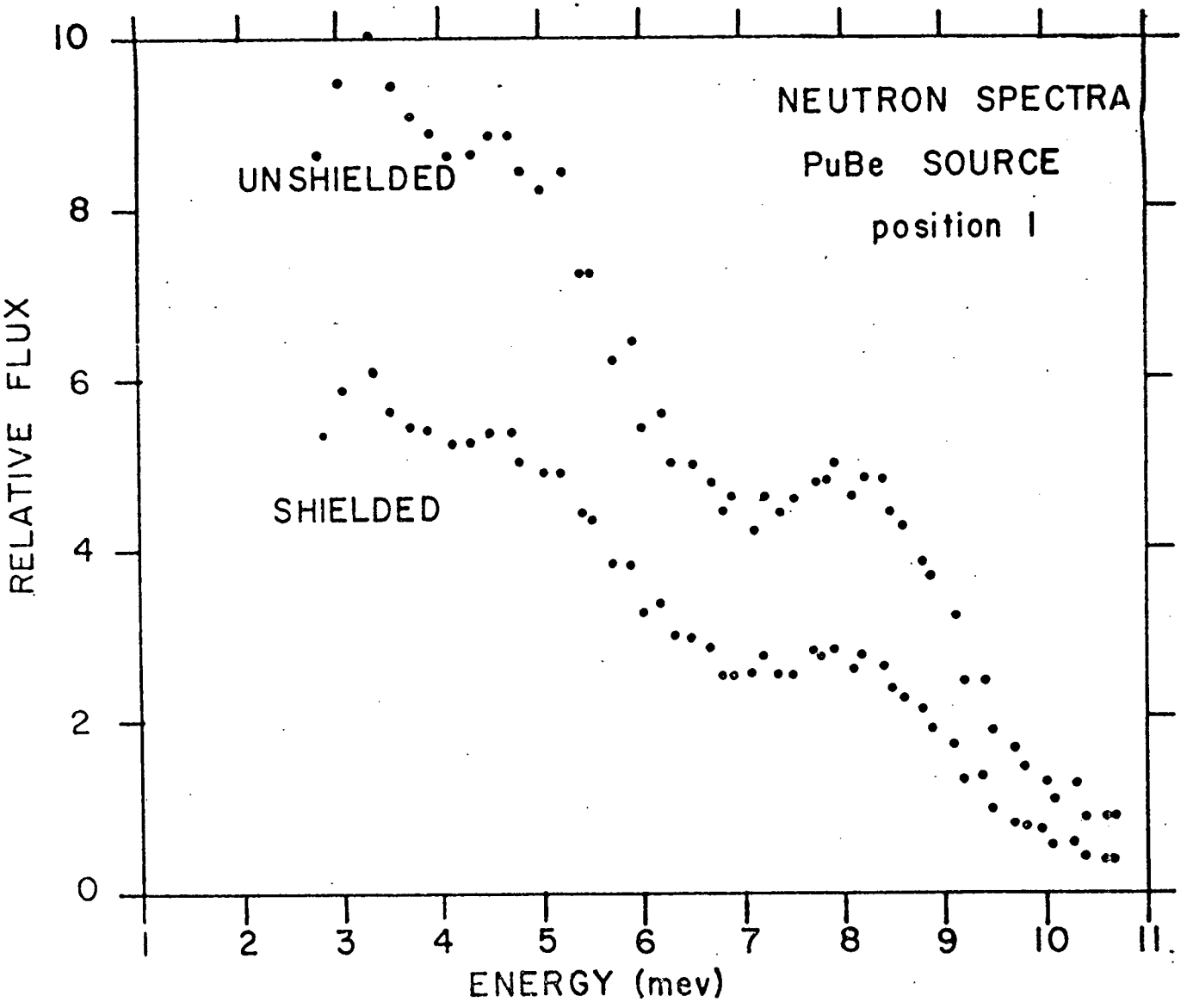
NEUTRON SPECTRA
PuBe SOURCE
position I
UNSHIELDED
SHIELDED
RELATIVE FLUX
ENERGY (mev)
0
2
4
6
8
10
1
2
3
4
5
6
7
8
9
10
11

FIGURE IV-4

D = detector

S = source

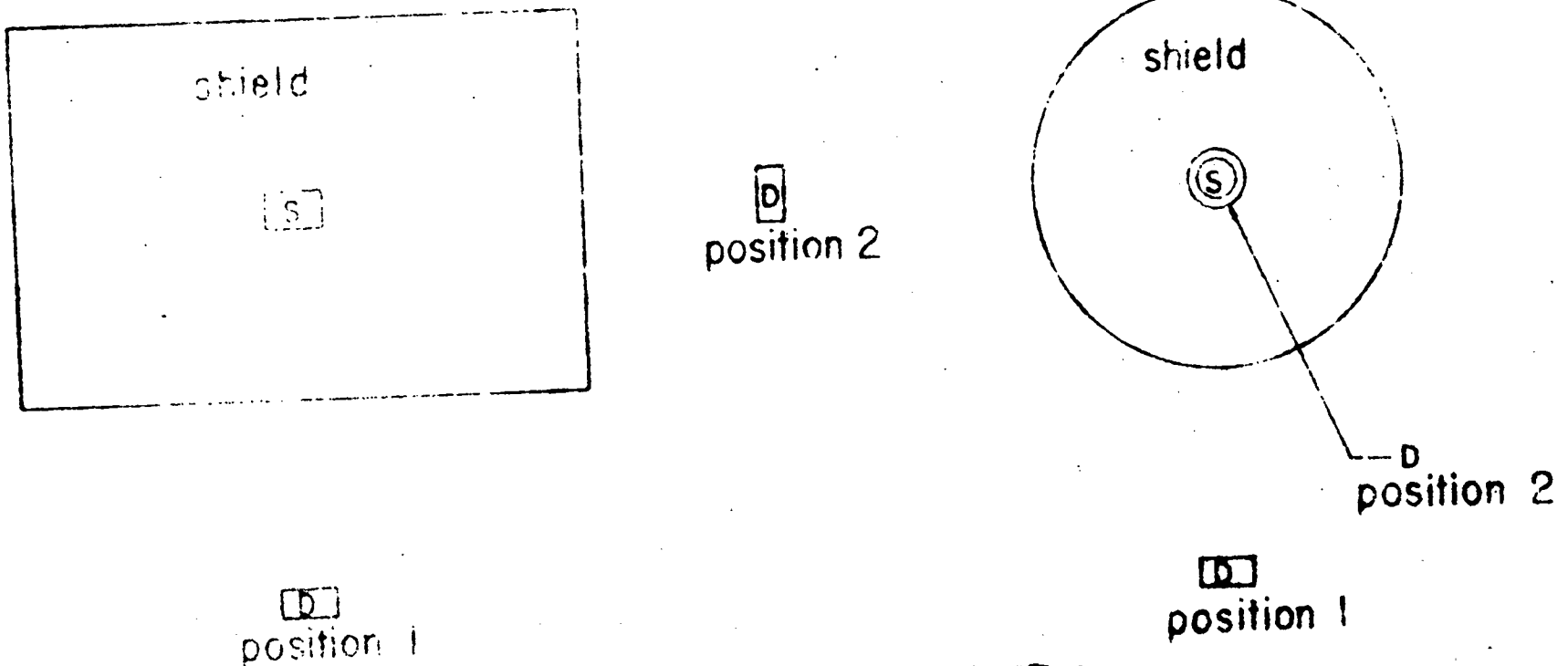

COUNTING GEOMETRY
(shown shielded)
no scale

FIGURE IV-5

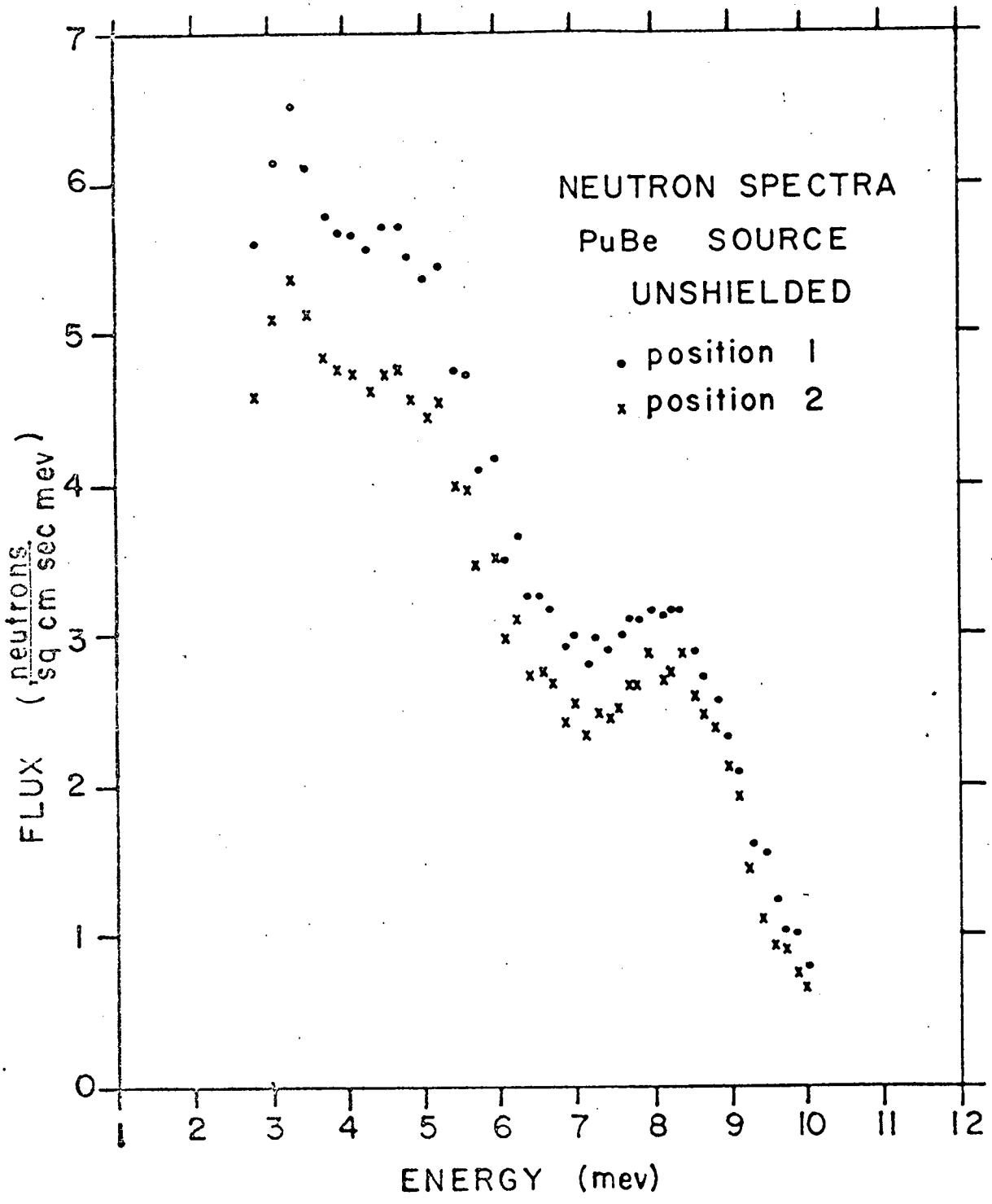
NEUTRON SPECTRA
PuBe SOURCE
UNSHIELDED
position 1
position 2
FLUX (neutrons / sq cm sec mev)
ENERGY (mev)
0
1
2
3
4
5
6
7
1
2
3
4
5
6
7
8
9
10
11
12

FIGURE IV-6

V. Neutron Spectrometer Simulation

D. Cunningham University of Wyoming
H. B. Eldridge University of Wyoming

In order to study the effects of various parameters upon the efficiency and resolution of the neutron time-of-flight spectrometer, a computer simulation of the system is being developed. In the simulation, the response of the organic scintillator to fast neutrons is being studied in detail. As nearly as possible all physical processes which occur within a scintillator exposed to a flux of neutrons are being considered and incorporated in the computer study. This model of the scintillator is then used for each detector in the simulation of the neutron spectrometer.

The physical processes which are to be included in the model of the organic scintillator are multiple (n,p) collisions and background occurring from inelastic and elastic scattering with other nuclei in the scintillator. A "good" collision occurs when a neutron scatters elastically from a proton and the neutron then escapes the scintillator after the one collision. If the neutron scatters from more than one nuclei before it escapes the boundaries of the scintillator, then a multiple collision occurs, and the first collision is no longer considered to be a "good" collision. The effect of multiple scattering in the scintillator is the following: since the time resolution of the electronics which collects the light output from the charged particles recoiling due to the multiple interactions of the neutrons with the media is finite, the instrumentation interprets the incident neutron to have been more energetic than it actually was. This effect is considered as background. The number of neutrons per incident flux of neutrons which undergo multiple collisions is measured in the simulation program as a function of incident neutron energy and orientation of the organic scintillator with respect to the source for NE102 and NE213, the results of which are illustrated in Figure V-1.

The largest part of the background occurring from collisions with other nuclei is the interaction of neutrons with carbon which has a nuclear density of the same order of magnitude as hydrogen in both NE102 and NE213. Because the light deposited in the scintillator from the interactions of neutrons with carbon is small in comparison with that deposited by recoil protons, the signal is generally below the discriminator level and can be ignored in the overall simulation of the system. However, the process must still be considered, since a collision with carbon is not a "good" collision and will decrease the efficiency of the scintillator in the detection of (n,p) scattering. Efficiency in this case is the number of "good" collisions which occur per incident flux of neutrons.

The response of the plastic scintillator as well as the efficiency is being studied. There is a coupling between the response and the efficiency of the scintillator and in order to optimize both the response and the efficiency, the dimensions of the scintillator must be large enough to gain maximum efficiency and small enough to eliminate the effects of multiple scattering. The edge effects is also a determining factor in the optimization of the parameters of the scintillator. If a recoil proton escapes the scintillator before all its energy has been deposited in it, then the instrumentation interprets this information to represent an incident neutron of lower energy than actually collided with the proton. The probability of the effect being significant is increased as the dimensions of the scintillator are decreased. Thus the optimization of both efficiency and response depends upon a sensitive balance of the parameters of the scintillator. The light output due to "good" collisions and multiple collisions occurring in a NE213 scintillator with incident neutrons of energy 2.0 MeV is illustrated in Figure V-2. The flux of neutrons is parallel to the x-axis, and normal to the y-z plane of the cylinder. The peaking at higher energies is due to the finite resolving time of the phototube and associated electronics viewing the scintillator.

The efficiency of the organic scintillator has been studied both as a function of composition and as a function of orientation. The two compositions considered were NE102, a solid plastic and NE213, a liquid scintillator. The efficiency was studied with the scintillator in two orientations. The first orientation was that with the symmetry axis of the cylinder parallel to the z-axis of the inertial system and the source of neutrons incident upon the curved surface of the scintillator. The second orientation studied was that with the symmetry axis along the x-axis of the inertial system and the source incident upon one of the flat surfaces of the cylinder. The results of these calculations are illustrated in Figure V-3.

The efficiency of the whole time-of-flight spectrometer as a function of energy is shown in Figure V-4. Neither multiple collisions nor background effects were considered in the preliminary model. The first scintillator is 2" X 2" and the second scintillator is 4" X 4". Both scintillators are NE102 composition. The second scintillator is set at a 45^{0} angle to the x-axis which extends through the source and the first scintillator. The flight path between the two scintillators is 1 meter long.

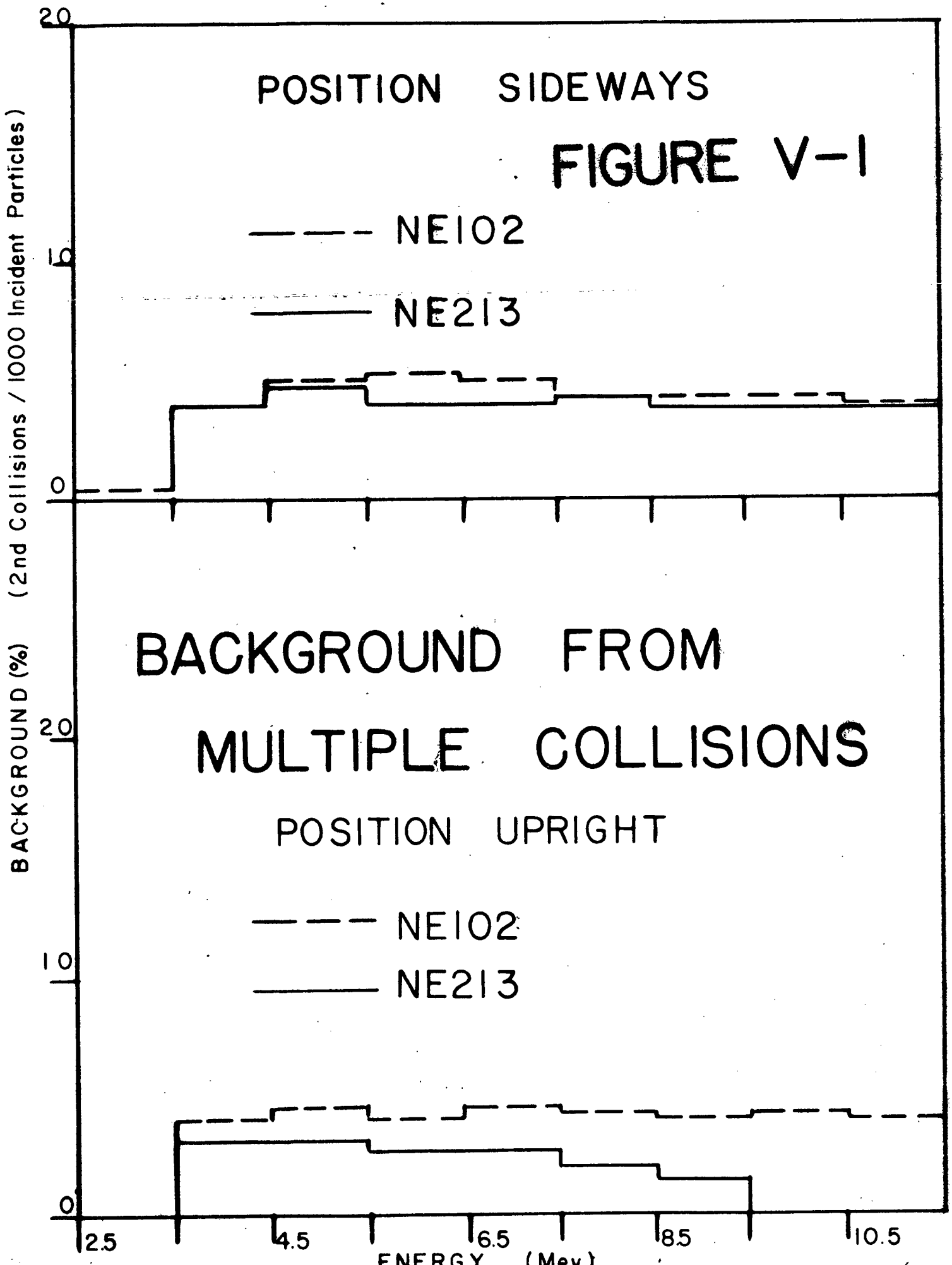
POSITION SIDEWAYS
FIGURE V-1
NE102
NE213
BACKGROUND (%) (2nd Collisions / 1000 Incident Particles)
20
10
0
BACKGROUND FROM
MULTIPLE COLLISIONS
POSITION UPRIGHT
NE102
NE213
2.5
4.5
6.5
8.5
10.5
ENERGY (Mev)

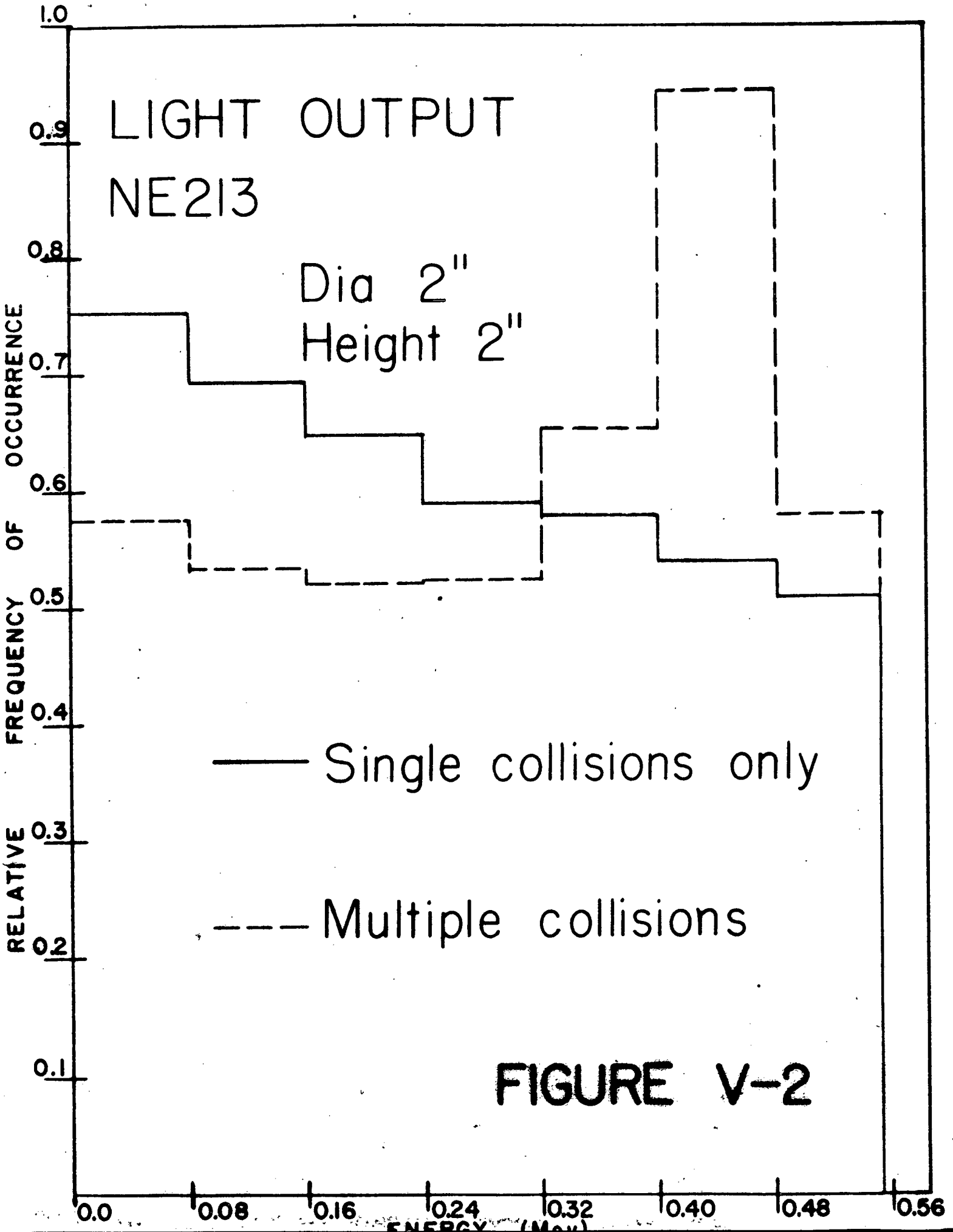
LIGHT OUTPUT
NE213
Dia 2"
Height 2"
Single collisions only
Multiple collisions
RELATIVE FREQUENCY OF OCCURRENCE
1.0
0.9
0.8
0.7
0.6
0.5
0.4
0.3
0.2
0.1
0.0
0.08
0.16
0.24
0.32
0.40
0.48
0.56

FIGURE V-2

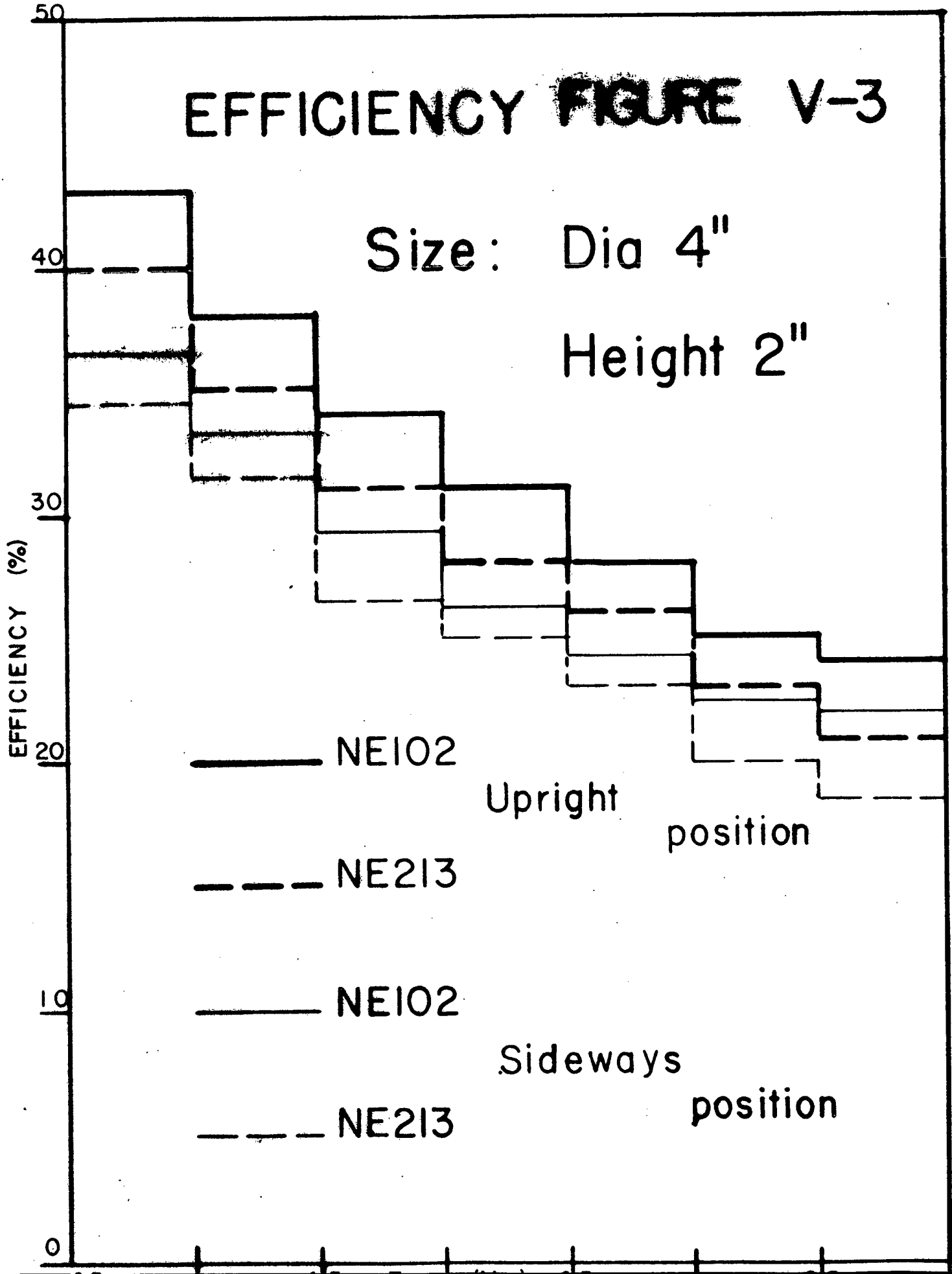
EFFICIENCY FIGURE V-3
Size: Dia 4"
Height 2"
50
40
30
20
10
0
EFFICIENCY (%)
NE102
Upright position
NE213
NE102
Sideways position
NE213

FIGURE V-4

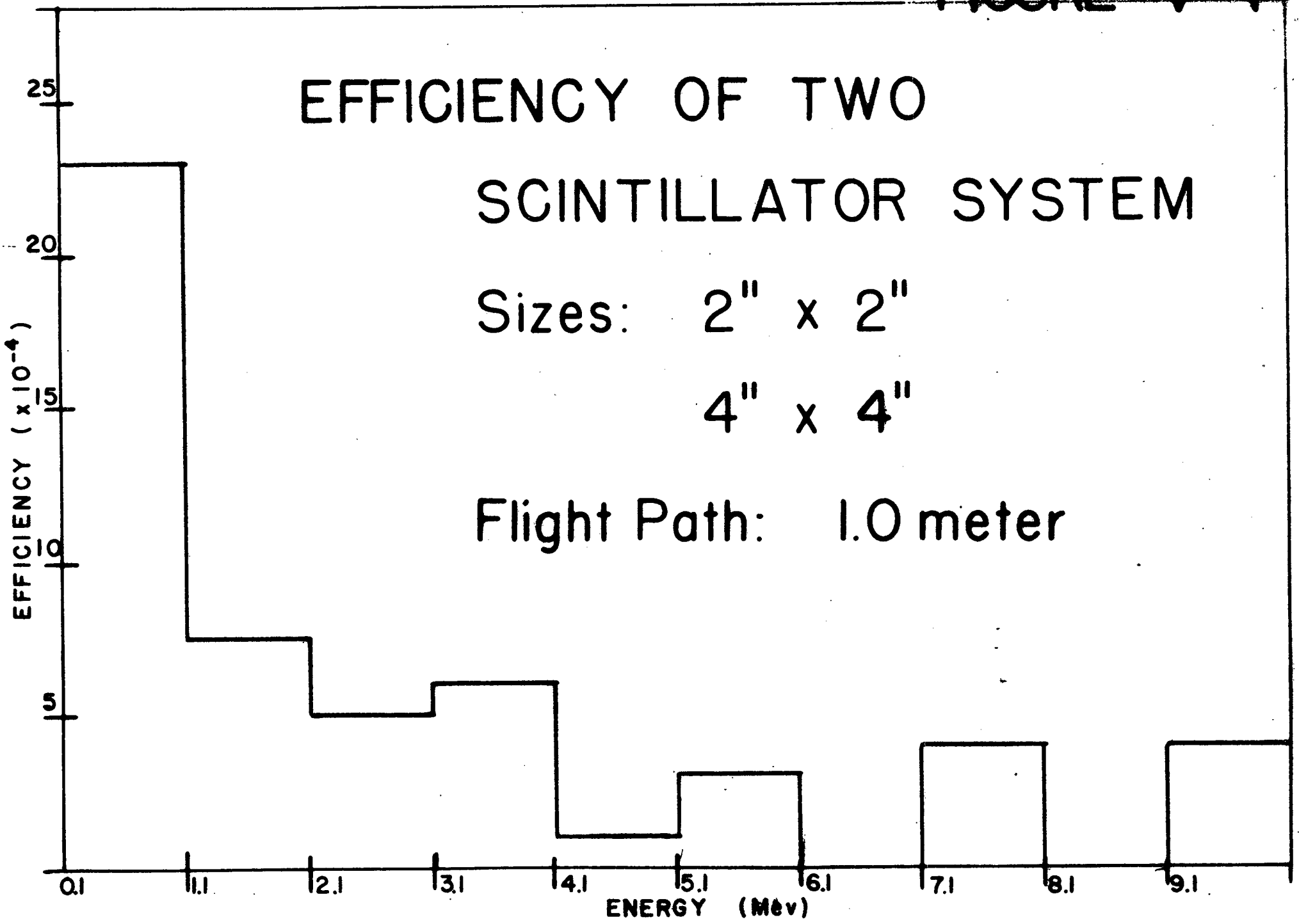
EFFICIENCY OF TWO
SCINTILLATOR SYSTEM
Sizes: 2" x 2"
4" x 4"
Flight Path: 1.0 meter
EFFICIENCY (x 10⁻⁴)
25
20
15
10
5
0.1
1.1
2.1
3.1
4.1
5.1
6.1
7.1
8.1
9.1
ENERGY (Mev)

VI. A Search for Germanium 64

L. Detch — University of Wyoming
H. Eldridge — University of Wyoming
C. Zaidins — University of Colorado
R. Dingus — University of Colorado

It has been suggested from am empirical observation that four particle clustering effects may play a more important role in intra-nucleon interactions than has been previously anticipated. In the following table the known even-even nuclei of total isotopic spin equalling zero are listed. The atomic mass number of these nuclei is an integer times four. It should be observed that for those nuclei listed as being stable, with the exception of Ar^{36}, the listed isotope has the most predominate natural abundance for that element. Those nuclei listed as being unstable, with the exception of Be^{8}, have longer half-lives than the next heavier isotopes which lie closer to the traditional "line of stability." This suggests that the nuclei of isotopic spin zero whose atomic mass numbers are integer multiples of four are in some sense preferred structures in nature or are more tightly bound.

n	4n	Nucleus	Half-Life	Natural Abundance	Next Heavier Isotope and Its Half-Life
1	4	He^{4}	Stable	100%	
2	8	Be^{8}	3×10^{-16} sec (alpha decay)		
3	12	C^{12}	Stable	98.9%	
4	16	O^{16}	Stable	99.8%	
5	20	Ne^{20}	Stable	90.9%	
6	24	Mg^{24}	Stable	78.7%	
7	28	Si^{28}	Stable	92.2%	
8	32	S^{32}	Stable	95.0%	
9	36	Ar^{36}	Stable	0.337%	
10	40	Ca^{40}	Stable	96.97%	

n	4n	Nucleus	Half-Life	Natural Abundance	Next Heavier Isotope and Its Half-Life	
11	44	Ti^{44}	47 years		Ti^{45}	3.08 hours
12	48	Cr^{48}	23 hours		Cr^{49}	42 min
13	52	Fe^{52}	8.3 hours		Fe^{53}	8.9 min
14	56	Ni^{56}	6.1 days		Ni^{57}	37 hours
15	60	Zn^{60}	2.1 min		Zn^{61}	89 sec
16	64	Ge^{64} (not yet observed)			Ge^{65}	1.5 min

From this empirical extrapolation one might expect to observe the existence of Germanium 64 with a half-life of the order of minutes to hours, or if this group of 4^3 nucleons is particularly tightly bound, perhaps by multiple clustering effects, the isotope could even be stable.

The proposed method of formation of Germanium 64 is by the reaction $Zn^{64}(He^3,3n)Ge^{64}$, using the 38 MeV He^3 beam of the Boulder Cyclotron (Colorado University) incident upon a Zn^{64} target. If Ge^{64} exists and is unstable, it should Beta decay to Ga^{64}. The gamma spectrum from Ga^{64} is not known but Ga^{64} decays to Zn^{64} by positron emission with a half-life of 2.6 minutes. The gamma spectrum of Zn^{64} is known and can be resolved using a Lithium drifted Germanium Solid State Detector, allowing the decay rate of Ge^{64} to be determined it is long compared with 2.6 min.

In the event that no activity which can be attributed to Ge^{64} is observed for Ga^{64}, the target may be conveniently chemically separated for Germanium and then mass-analyzed for Ge^{64} using the mass separator at the Boulder Cyclotron Laboratory.

Preliminary runs indicate that the several lines in the Zn^{64} decay scheme resulting from Zn^{64} bombardment with He^3 can be resolved sufficiently to measure the decay rate. This run also allowed a rather loose lower limit to the half-life of Ge^{64} to be set as greater than 30 minutes. Experimental difficulties have prevented an immediate follow up of this result.

VII. Energy and Angular Distributions of Neutrons Emitted from the Interaction of 160 MeV O^{16} Ions with Nickel and Silver

W. G. Simon and S. T. Ahrens

The data, as described in the previous progress report, show a prominent backward peaking in the center-of-mass system. We have interpreted this peaking as a result of the transfer of only part of the incident O^{16} ion to form a compound system. This compound system, which is moving backward in the center-of-mass system, evaporates particles that are backward peaked. We have used the data of Pfohl[1] obtained by direct observation of reactions of Ne^{10} ions with emulsion nuclei, to estimate the number of transfer reactions occurring. We assume that complete fusion of the O^{16} with the target nucleus occurs 60% of the time, the transfer of a C^{12} occurs 10% of the time, and the transfer of an alpha particle occurs 30% of the time. In each case the particle not transferred continues without breakup or change in velocity. These reactions are considered to be reasonably representative of the larger set of reactions actually observed by Pfohl.

Calculations of the spectra of particles evaporated from the resulting heavy, excited nuclei are done with the aid of a modification of a computer program written by D. V. Reames.[2] These include the effects of angular momentum and multiple particle emission. Multiple emission is considered approximately in the following way. A first chance spectrum is calculated. This includes the evaporation of all types of light particles being considered. An average residual nucleus is arrived at by averaging over the energy, angular momentum, charge and mass removed from the system. This residual nucleus then evaporates a second chance particle and a new average residual nucleus is calculated for third chance emission. This process proceeds until particle emission is no longer energetically possible. Particle spectra resulting from systems formed in transfer reactions are then transformed to the center-of-mass of the entire system, where comparisons are made. Figure VII-1 shows the results of

these procedures. The upper curve represents the 4-MeV meutron angular distribution resulting from the complete fusion of the O^{16} nucleus with the target, assumed to occur with total cross section equal to 60% of the reaction cross section. The lower two curves represent the angular distributions resulting from alpha transfer (30% of the reaction cross section), and from the transfer of a C^{12} Nucleus (10% of the reaction cross section). The sum of these three distributions is our prediction for the angular distribution of neutrons and is shown in Figure VII-2 along with our experimental data. The calculatings do not show as much backward peaking as observed. However, owing to the many approximations in the calculations, it appears unreasonable to attempt any more than a qualitative explanation of the asymmetry. As pointed out by Reames, a shortcoming of the evaporation calculations exists which could greatly underestimate the 0^{o} to 90^{o} asymmetry of low energy particles. In calculating level densities, an expansion is made in U_R /U (the rotational energy over the total excitation energy of the nucleus) in which only the lst order term is kept. Particle emission is "inefficient" in removing angular momentum from a nucleus. After several particle emissions occur U_R may comprise a major part of the total excitation energy and the expansion is poor. The result is that asymmetries for low energy particles emitted near the end of the evaporation chain are underestimated. An increase in the calculated cross sections at both 0^{o} and 180^{o} would improve the agreement. The assumption of large cross sections for transfer reactions without an increase in the total reaction cross section results in a normalization discrepancy. We are trying to understand this discrepancy by examining the total energy carried away by particles and gamma rays and comparing this with the energy assumed to be brought into compound systems by both the total fusion reactions and transfer reactions.

---

1. Raymond Pfohl, "Reactions Nucleairs Provoquees Les Interactions Du ^{20}Ne De 200 MeV Avec Les Noyaux De L'Emulsion Ionographique," De L'Universite De Strasbourg, thesis (unpublished).

2. Donald V. Reames, Phys. Rev., 13137, 332 (1965).

FIGURE VII-1

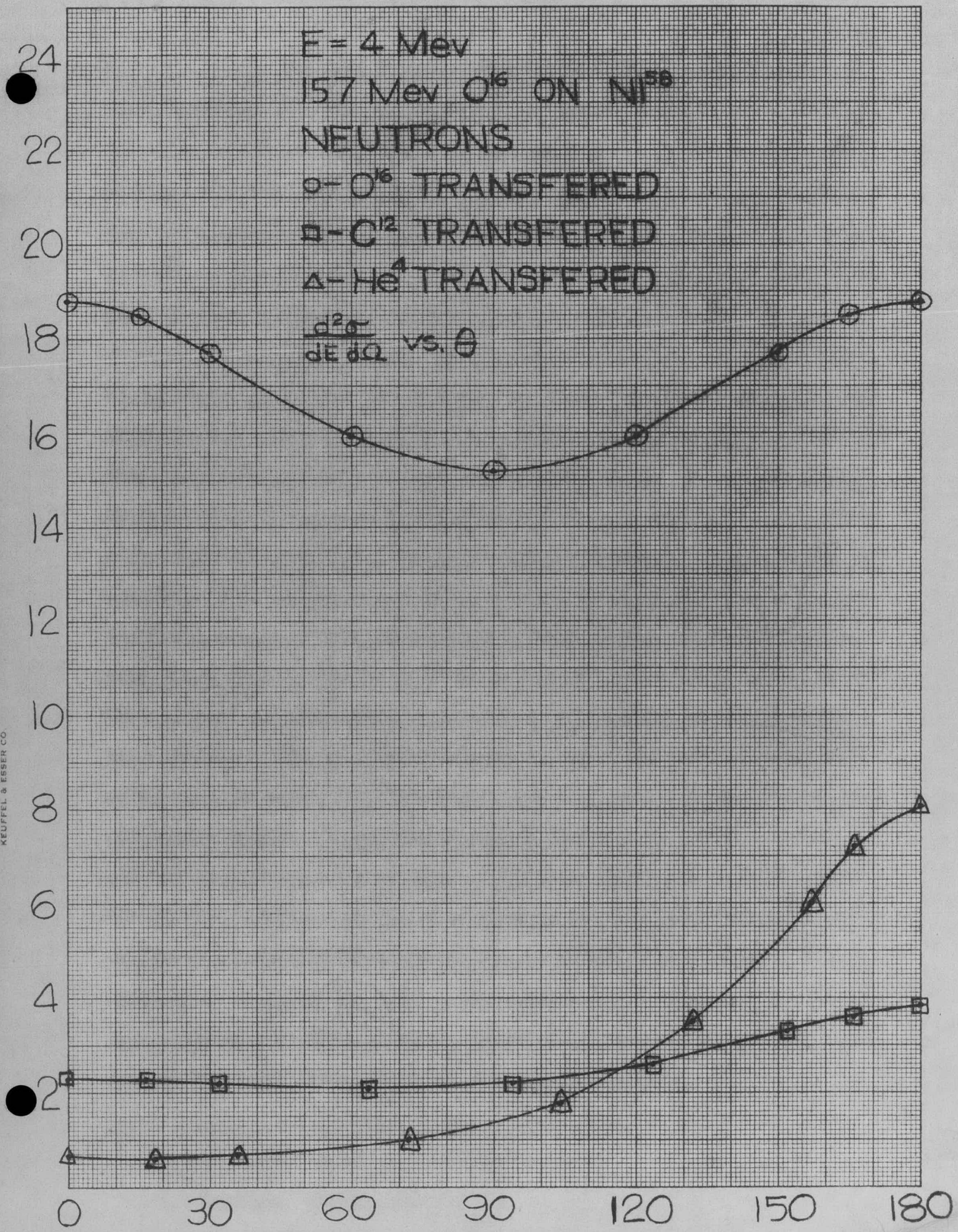

FIGURE VII-2

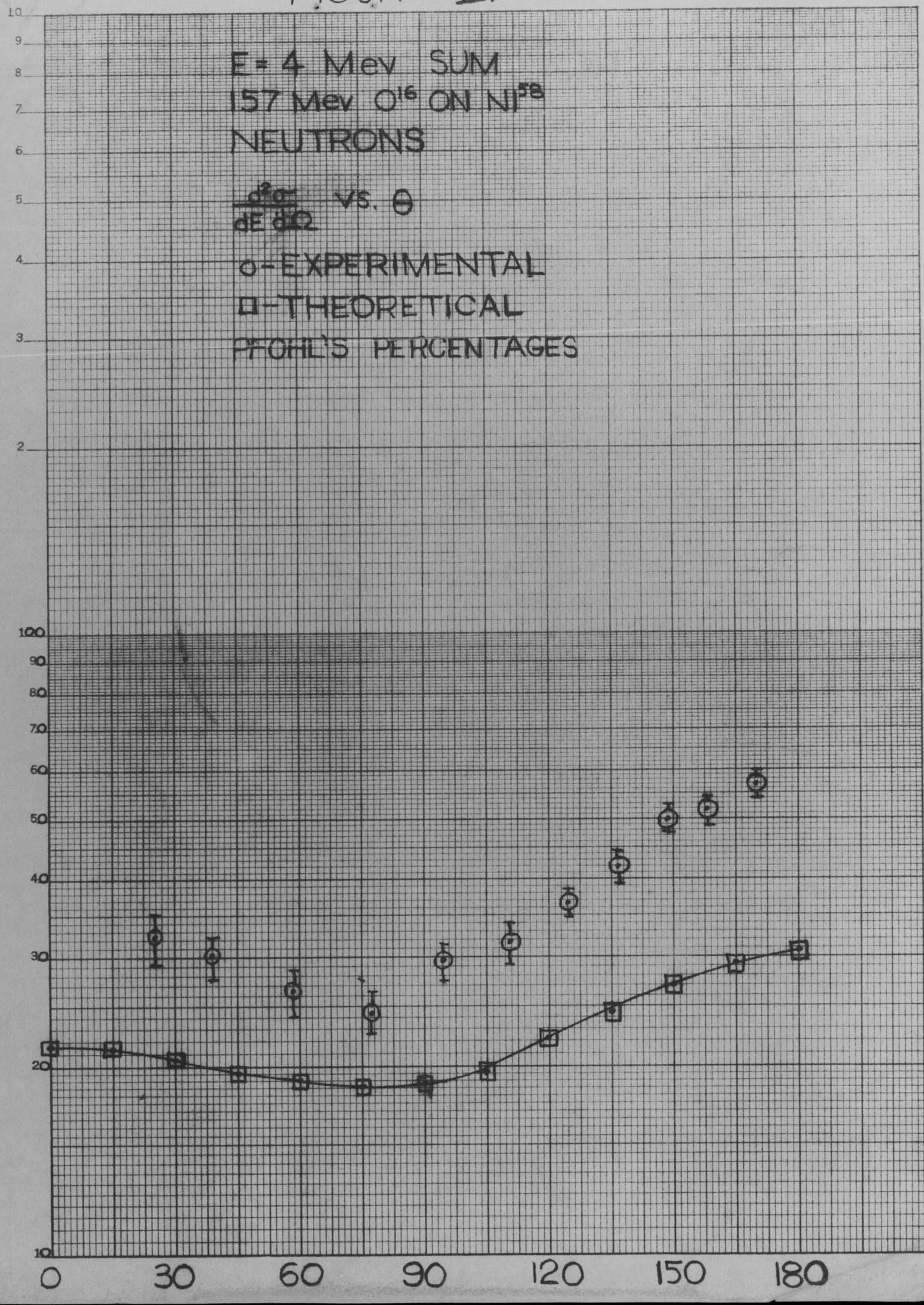
E = 4 Mev SUM
157 Mev O^{16} ON NI^{58}
NEUTRONS
$\frac{d^2\sigma}{dE\,d\Omega}$ vs. θ
o-EXPERIMENTAL
□-THEORETICAL
PFOHL'S PERCENTAGES
10
9
8
7
6
5
4
3
2
100
90
80
70
60
50
40
30
20
10
0
30
60
90
120
150
180
SEMI-LOGARITHMIC 46 5132
2 CYCLES X 140 DIVISIONS MADE IN U.S.A.
KEUFFEL & ESSER CO.

VIII. Personnel

Academic and Scientific Staff

Name	Position
H. B. Eldridge	Assistant Professor
W. G. Simon	Associate Professor

Support Staff

Name	Position
K. Billings	Secretary
J. Burnett	Emulsions Scanner
B. Long	Emulsions Scanner
N. Ghaddis	Emulsions Scanner
G. Shipp	Emulsions Scanner
J. Thomas	Machinist

Research Assistants

S. T. Ahrens

D. L. Cunningham

L. Kroger

J. Shideler

Undergraduate Students (part time)

T. Meyer

Y. Takamori

R. Hunt